Proc. Natl. Acad. Sci. USA
Vol. 76, No. 7, pp. 3051–3055, July 1979
Geophysics

Determination of water mass properties of water pumped down from the Ekman layer to the geostrophic flow below

(subtropical gyre/Ekman pumping/water mass origins)

HENRY STOMMEL

Woods Hole Oceanographic Institution, Woods Hole, Massachusetts 02543

Contributed by Henry M. Stommel, April 6, 1979

ABSTRACT **In a subtropical gyre, the convergent Ekman layer forces water downward into the geostrophic flow below. The properties and depth of the mixed layer vary considerably during the course of the year, but this variability does not penetrate into the geostrophic region. Evidently there is some process at work that selects only late winter water for actual net downward pumping. It is a process much like that performed by Maxwell's Demon. Arguing from a particular example in a North Atlantic region where Sverdrup dynamics is presumed to prevail, an elementary description is given as to how the Demon works and a sample set of profiles by season is computed. Present day mixed layer models involve a local vertical mixing process. Thermocline theories involve adiabatic flow from high latitudes. There is an intermediate depth range at which the two processes operate alternatively, according to season.**

Elementary discussions of the ocean circulation often begin with a description of how, in a vertical meridional plane, density surfaces rise to the surface successively in the manner shown in Fig. 1. Two regimes are envisaged: a surface mixed layer, which contains the Ekman dynamics, and a deep geostrophic regime below. Where this section passes through a subtropical gyre, the Ekman transport is convergent, as shown, and this forces water downward from the mixed layer into the geostrophic regime below, leading to a circulation in the meridional plane as sketched in the figure. In the geostrophic regime, there is also little flow across density surfaces.

Although it is tempting to assume two-dimensionality, by making everything independent of longitude, this would restrict the geostrophic flow to the zonal component (an eastward relative surface flow). We would encounter difficulty in explaining the meridional components of flow in the geostrophic regime shown in Fig. 1.

If, on the other hand, we make our description consistent with Sverdrup dynamics, then we should pivot our conceptual model on strong meridional components of geostrophic velocity, and admit the necessary east–west dependence. Because of its simplicity, a region of Sverdrup dynamics should be a favorable place to trace and explain the paths of water being forced downward by Ekman pumping. We are therefore faced with the problem of finding a region where Sverdrup dynamics prevails.

Doubts about the universality of Sverdrup dynamics in the open ocean were the main reason for initiating the MODE program in 1970, and it now seems certain that large non-Sverdrupian regions are common. However, recent studies (1, 2) suggest that eastern portions of the subtropical gyres may be predominantly Sverdrupian. A region southwest of the Azores, centered at about 28°N 36°W has been identified as probably Sverdrupian by means of the "beta-spiral" calculation and has been chosen for further field studies. Because of the determinations of absolute geostrophic velocity field and of the estimated vertical component of velocity in this region and because of new data that are presently being obtained there, it is a convenient location in which to make our study.

A further convenience is that this region lies within a larger region already the subject of a classic study by Montgomery (3), who demonstrated that between 0° and 30°N it is plausible to trace water forced down from the Ekman layer into the geostrophic, adiabatic flow regime below. He provided a descriptive picture of the circulation, assuming that it is confined to isentropic surfaces and flows in a direction indicated by the orientation of tongues of isohalines. Montgomery attached an approximate magnitude to the currents by a geostrophic velocity calculation using a line of *Atlantis* (March 1932) stations near the 40th meridian. Montgomery's descriptive analysis is fully compatible with the physical ideas involved in the "beta-spiral" diagnostic calculation and with the concept of a simple linear Sverdrup regime. My present study extends Montgomery's study in two ways: first, it introduces the Sverdrup dynamics and, second, it treats the seasonal variability.

The basic description is a steady-state dynamical one. For a first quantitative pilot calculation of water flow, we will first suppose that the only water that escapes downward from the mixed layer is that corresponding to late winter conditions when the mixed layer is deepest. In view of the large annual range of variability of the depth and temperature of the mixed layer, this steady-state assumption requires an explanation, which I offer after the steady-state presentation.

During October–November 1978, the *R/V Eastward* made 30 pairs of hydrographic and expendable bathythermograph stations along the sides of the triangle $\overline{ABC}$ shown in Fig. 2. The direction of geostrophic flow relative to 1000 m (Fig. 3) at 200 m in this region is roughly perpendicular to side $\overline{BC}$.

According to the Böhnecke (*Meteor*) Atlas, there is a broad (≈225 km wide) band, in February, of water in the mixed layer with temperatures between 20°C and 21°C lying northeastward of and parallel to side $\overline{BC}$. Evidently, when forced downward out of the mixed layer, this 20°–21°C water flows across the face $\overline{BC}$, well submerged below that of the mixed layer there at any time of year. The data obtained on the *Eastward* indicates that the layer of 20°–21°C water on face $\overline{BC}$ lies at a depth of about 150 m and a vertical thickness of about 24 m, corresponding to the configuration shown in Fig. 4. Fig. 4 is a specific example of the general picture already given in Fig. 1. From the various determinations (2) of absolute velocity already made in this region, it seems likely that the normal component of velocity at 150 m across the face $\overline{BC}$ is about 0.9 ± 0.1 cm sec^{-1} toward 205°T (T, true).

In this picture, the configuration of the flow field is approximately independent of the direction 115°T, normal to the plane of the figure. This permits us to make a two-dimensional

The publication costs of this article were defrayed in part by page charge payment. This article must therefore be hereby marked "*advertisement*" in accordance with 18 U. S. C. §1734 solely to indicate this fact.

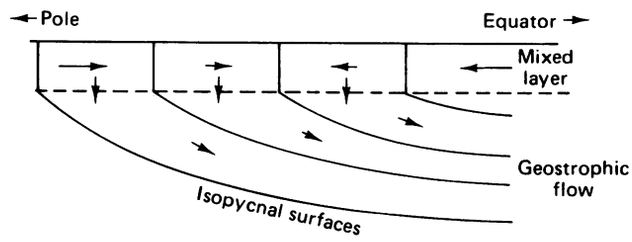

FIG. 1. Schematic representation of flow in meridional plane showing convergent Ekman layer pumping water down into deep flow along isopycnal surfaces.

calculation for the Ekman pumping w by continuity:

$$w = \frac{24\text{ m}}{225 \times 10^3\text{ m}}(-0.9\text{ cm sec}^{-1})$$
$$= -9.6 \pm 2 \times 10^{-5}\text{ cm sec}^{-1}.$$

The estimates of Schott and Stommel (2) of w from beta-spiral calculation are in a range of from -10.1 to -15.0×10^{-5} cm sec^{-1}, which is consistent with the value from continuity.

The above estimates of w are independent of any data on the distribution of wind stress. Using wind reports from ships, Leetmaa and Bunker (1) have computed mean downward fluxes in rectangular areas 2° of latitude by 5° of longitude. The area 26°–28°N, 30°–35°W has a downward Ekman flux of 0.09 Sverdrups; surrounding areas average 0.20. We may therefore take the range of upward velocities at the base of the Ekman layer in the triangular area of Fig. 1 to be between -8.2 and -18.0×10^{-5} cm sec^{-1}. It is unfortunate that there is such a spread in values here. The larger value is representative of more squares, and Leetmaa claims to be puzzled about the single low value of -8.2. In any case, however, our value of w falls within the range of uncertainty of the Leetmaa–Bunker tabulations. It does seem to indicate that the Sverdrup regime traces the water masses downward correctly.

The foregoing calculation has been done assuming that the temperature and salinity of the water pumped downward essentially corresponds to that which occurs at the time of year of the deepest mixed layer depth; but the temperature and depth of the mixed layer are strong functions of latitude and time of year. According to Böhnecke's *Meteor* Atlas, surface temperature in the area (at 25°N 35°W) ranges from a low of 21.5°C in March to 25.6°C in September. The mixed layer depth varies locally from approximately 100 m in February to

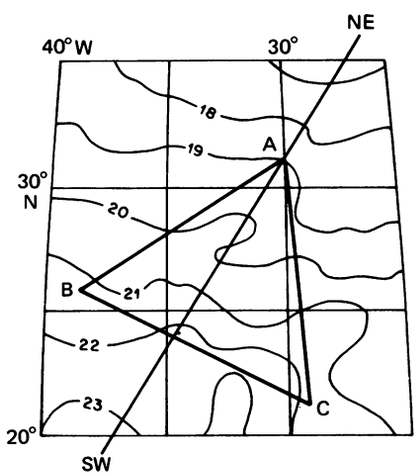

FIG. 2. February sea surface temperatures (°C, *Meteor* Atlas), showing triangle of stations.

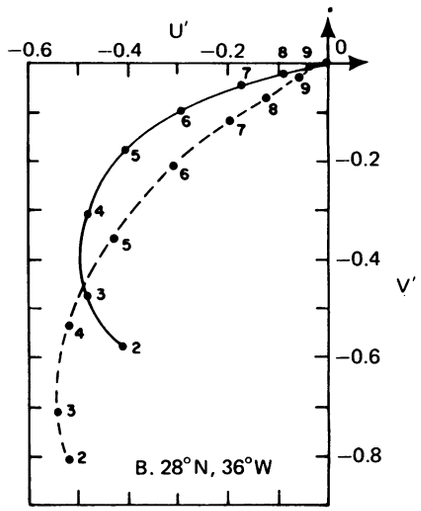

FIG. 3. Relative geostrophic velocity at point B. Two data sets, solid and dashed, both International Geophysical Year (IGY) data.

less than 50 m in August. It is clear that in late summer locally the mixed layer is pumping water downward with a temperature 5°C greater than in late winter, but at a shallower depth. There is only a small local seasonal variation of mixed layer salinity. Looking at the problem another way, we may ask to what latitude the 20.5°C mixed layer temperature has moved in summer, and we can see, from either the Böhnecke charts or the monthly vertical temperature section along 30°30′W drawn by Schroeder (4) (and reproduced in Fig. 5), that in September it is as far as 45°N. Thus, we see that there is a problem: if the deep geostrophic regime is to be regarded as steady in time, how can this be consistent with a source of supply whose temperature fluctuates so much? Let us begin then by assuming that the flow pattern beneath the mixed layer is steady with time. In this case, as calculated above, geostrophic flow lines beneath the mixed layer slope downward toward the south in the NE–SW vertical plane with a slope of about 10^{-4}. With some small logical inconsistency, a streamline ψ with the same slope has been drawn on the Schroeder sections along 30°30′W through the point (25°N, 100 m depth). It is convenient, as a point of departure, to argue that the direction and speed of flow downward in the geostrophic region below the mixed layer is constant in time. Such a hypothesis certainly needs future reexamination and justification; at present we use it as a tool to take a preliminary look at the distribution of sources of water supply.

On Fig. 5, we also mark, by a short horizontal line segment, the point P at which the mixed layer depth intersects the streamline ψ. For clarification, this construction is also drawn schematically in Fig. 6. This point P moves north and south during a year, according to Fig. 5, oscillating between 25°N and 35°N. The north–south movement of the 20.5° isotherm in the

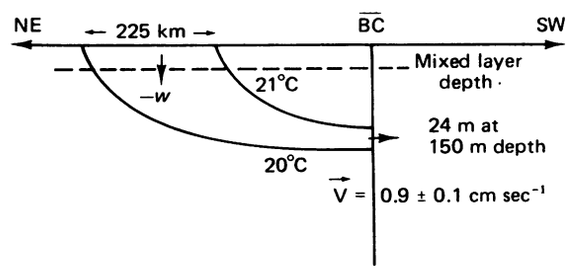

FIG. 4. The 20°–21°C water mass being transported downward from the Ekman layer and across vertical section $\overline{BC}$.

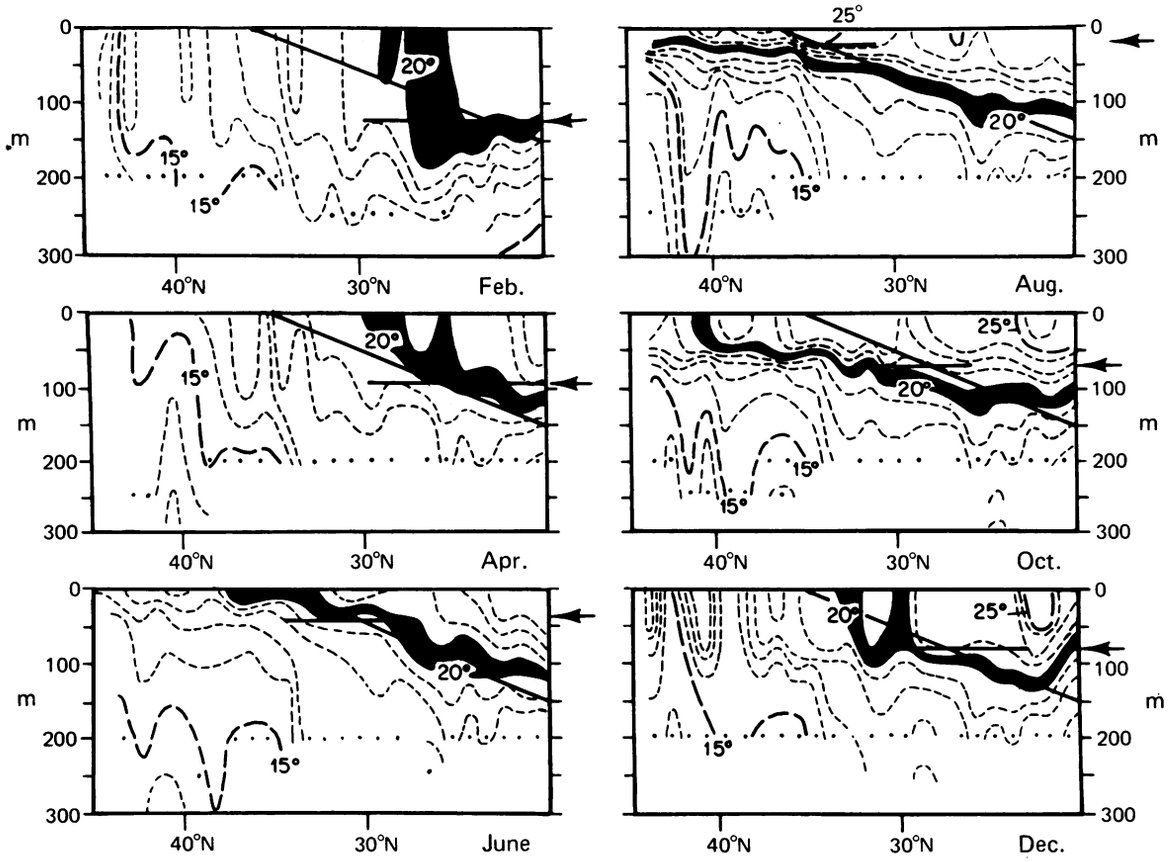

FIG. 5. The 20°–21°C water layer on 30°30′W meridional plane during different months of year (4). Oblique line has slope of 10^{-4}; horizontal segment shows mixed layer depth.

mixed layer is about twice as large: the amplitude of meridional migration of isopycnals is even greater.

If we examine Fig. 5 to discover the temperature of the water pumped down past point P each month, we can see that from February to June, the point P moves at a northward rate which tends to be isothermal; during this whole period, the supply of water to the streamline ψ remains at almost constant temperature 20.5°C (but of course rapidly dropping salinity). From July through February the point P moves southward again, at a rate of 10° latitude in 5 months at about 7.3 cm sec^{-1}. Since this is much larger than the average southward rate of geostrophic flow along ψ, it is clear that in its southward advance the moving point P is actually "swallowing up" water pumped onto ψ earlier in the year so that by the time P reaches its southern limit at 25°N, the only water that has not been swallowed up is that pumped onto ψ during the early spring season, which has now moved south of 25°N. Thus, despite the large fluctuations of temperature and salinity that occur on the moving P during the course of the year, they do not penetrate down south of 25°N on ψ. A very much restricted range does. The water that escapes southward of 25°N along ψ each year has never had an origin north of 27°N, its temperature has not varied by as much as 1°C, and its salinity has varied correspondingly little.

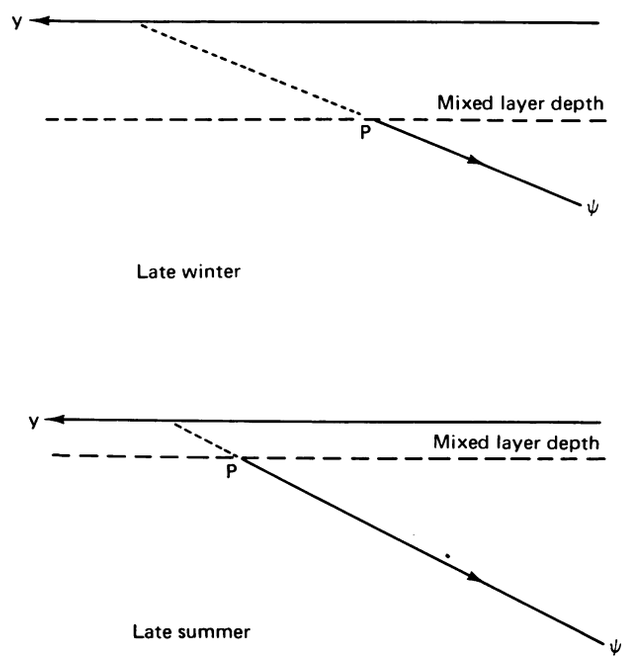

FIG. 6. Oblique movement of the intersection P of the fixed streamline ψ and the bottom of the mixed layer, in the vertical meridional plane.

The process can be followed in detail in Fig. 7, in which the abscissa is time of year, starting perhaps in February, and the ordinate is y, a north–south coordinate along the NE–SW line. The heavy curve y_i is the position of the point P where the mixed layer (which itself moves up and down throughout the year) intersects the streamline ψ.

The short arcs, $t_0, t_1, \ldots$, are the y positions of the isotherm in the mixed layer as a function of time of year. The y amplitudes of curves of constant t_i are larger than that of y_i and, hence, shown as small arcs. The temperature t_i that intersects the curve y_i is the instantaneous value of temperature right at the bottom of the mixed layer being pumped down the inclined

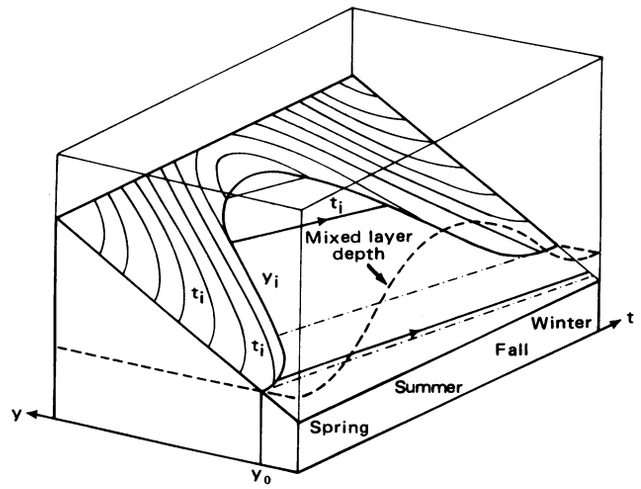

FIG. 7. y,z,t space, showing streamplane, mixed layer depth, their curve of intersection y_i, and trajectories of constant temperature.

line. Because the flow down the inclined line is taken as steady, the temperatures slope uniformly down toward the south in those positions of the plane between y_i and y_0, being warmer in the north. As can be seen, many of these lines of constant temperature also intersect the curve y_i again in the fall, where the rapidly deepening mixed layer overtakes the warm water flowing south. Only those isotherms that pass below minimum of y_i at the end of winter can pass into the permanently geostrophic region south of y_0. Thus, there is only a small range of temperature from t_0 to t_1 being pumped southward along the plane, and only a small range of salinity as well. (The north–south amplitude of isohalines in the mixed layer is very small compared to that of isotherms.) As a result, the only properties being pumped downward into the upper main thermocline are the temperature and salinity values corresponding to late winter and early spring mixed layer values.

An alternative calculation sheds some light on the seasonal variation of properties beneath the mixed layer. We cannot regard the vertical distribution of properties as the result of a purely one-dimensional vertical process. At all depths beneath the mixed layer, the properties depend upon equatorward advection, from the base of the mixed layer further poleward, and they may involve some degree of time variability.

The calculation can be made clear by application to our test location 25°N 35°W. In Fig. 8 we have drawn schematically a sloping streamline ψ in the vertical meridional plane, with uniform slope S, along which we envisage a constant southward flow with horizontal component equal to the constant V. The depth of the mixed layer is $D(t)$ and its temperature is $T(y, t)$. At point y_0, the temperature profile is made up of the following

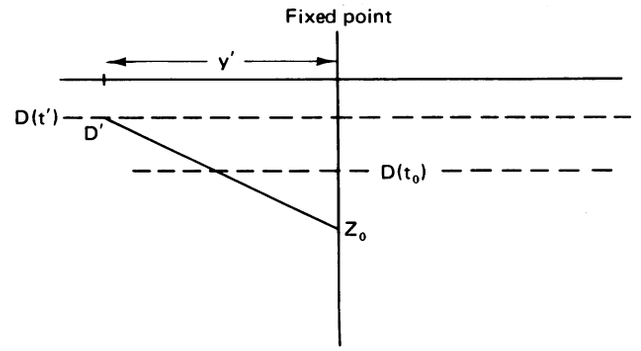

FIG. 8. Geometry of the x,y plane.

parts (z being measured positive downward): part 1, $0 < z \leq D$, $T = T(y_0, t)$, a quantity that is fixed; and part 2, $D < z$, here for T we must move up the appropriate streamline ψ until we encounter its last intersection with the mixed layer. For concreteness, let us choose the origin of time t at the coldest time of the year and the position of the station where we want to compute $T(z, t)$ at $y = 0$. The depth of the mixed layer may be taken as $D(t) = D_0 + E \cos 2\pi t$ and the temperature of the mixed layer $T(y, t)$ as $T = T_0 - By - C \cos 2\pi t$. If we choose, at $y = 0$, a particle of water at a depth z and time t, we can compute the previous coordinates of the particle when it left the mixed layer, y', z', t', by the formulas

$$z' = z(t) - SV(t - t')$$

and

$$y' = (t - t')V.$$

The time t', when it last intersected the bottom of the mixed layer, comes from the condition

$$z'(t') = D(t') \text{ for least } (t - t'),$$

the temperature then being

$$T' = T_0 - By' - C \cos 2\pi t'.$$

For our point at 25°N 36°W we may take the following parameters starting at March 1: $T_0 = 23°C$, $C = 2°C$, $S = 10^{-4}$, $B = 1°C/230$ km, $D_0 = 0.050$ km, $E = 0.050$ km, and $V = 360$ km yr^{-1} if time t is measured in years and y in km. Let us compute the profile for time t_0. First we must find t' for a given z:

$$0.05 \cos 2\pi t' + 0.05 - z + 0.360\,(t_0 - t') = 0.$$

By iteration, we find t' for least $(t_0 - t')$. Then calculate

$$y' = (t_0 - t')\,360$$

and then

$$T' = 23 - \frac{1}{230} y' - 2 \cos 2\pi t'.$$

From these formulas the local soundings of temperature and salinity can be reconstructed as functions of time of year. Fig. 9 is such a construction at $t_0 = 0$, 0.25, 0.50, and 0.75 years, the origin being taken at the end of February, when mixed layer depth is greatest and temperature lowest. The temperature sounding shows us a noteworthy feature: the structure in the depth interval between the mixed layer at its instantaneous value and its deepest value layer (100 m in this case) at any time is remarkably constant in time, with a vertical gradient very much the same as that in the permanently geostrophic regime below. In this depth interval the temperature does change with time, but only as a clipped cosine wave, as shown in Fig. 9. The temperature soundings beneath 100 m show some small variability in time, generally less than 0.1°C. By contrast, the salinity profile in Fig. 9 exhibits a series of annual steps propagating downward, each nearly homogeneous, of about 36 m in thickness.

In nature, there would be instability at these sharp salt interfaces; some mixing, which we could anticipate, will largely wipe out the steps, first by gravitational instability and then perhaps by a slower salt-finger process. The resulting deep sounding then must be approximately

100 m	21.0°C	37.2 ‰
150 m	18.8°C	36.9 ‰
200 m	16.7°C	36.5 ‰

which corresponds to the temperature–salinity relationship

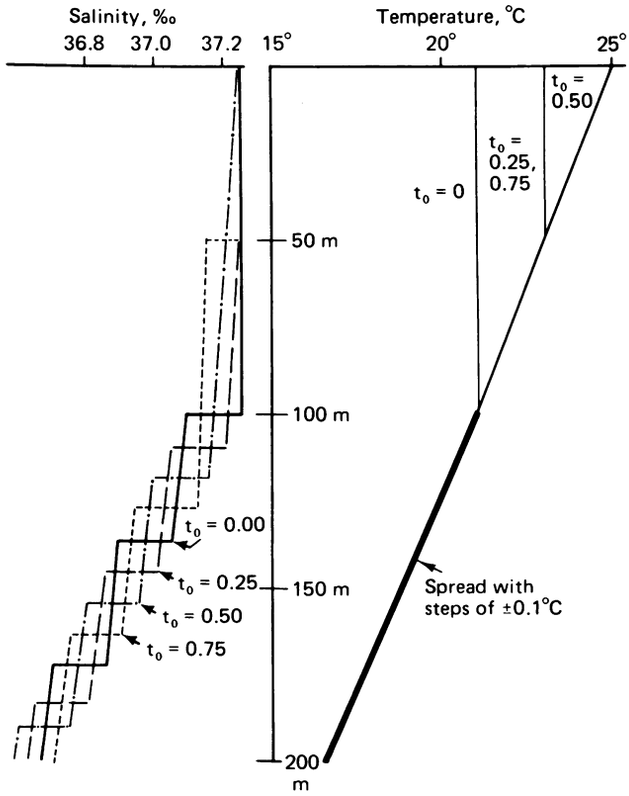

FIG. 9. Computed temperature and salinity profiles at a fixed point for different seasons of year. t_0 = 0.00 corresponds to March 1.

present in the mixed layer in late winter. Summertime mixed-layer properties never penetrate deeply down into the permanently geostrophic layer even though, in this construction, they are being pumped down all year round because they are overtaken by the rapidly deepening mixed layer of autumn and early winter.

The fact that, in this computation of vertical soundings, deep temperature is continuous but salinity is stepped depends upon choice of parameters; temperature could easily be slightly stepped. Too much importance should not be attributed to the more or less adventitious character of these microfeatures; the important point is that high summertime temperatures never manage to escape into the deep water, *despite the fact that they are pumped downward*, because they are overtaken on the way down (and southward) by the rapid autumnal deepening of the mixed layer.

The soundings are not computed beneath 200 m in depth because at this depth the origin of the advective layer is as much as 1000 km to the north and so great a distance begins to stretch the credibility of the simple linear extrapolation nature of the model. To extend the calculation further horizontally one would need to take into account the horizontal changes of direction of flow in the gyre, the changing orientation of surface isotherms, the geographical variability of Ekman pumping, etc. To calculate more deeply also would involve allowing for rotation of the geostrophic velocity with depth and a diminishing vertical component of velocity; in other words, we would need a model for the whole gyre, not just a small linearized portion of it.

This work was supported by Grant OCE78-18460 of the National Science Foundation. This is Woods Hole Contribution 4351.

1. Leetmaa, A. & Bunker, A. F. (1978) *J. Mar. Res.* **36**(3), 311–322.
2. Schott, F. & Stommel, H. (1978) *Deep-Sea Res.* **25**, 961–1010.
3. Montgomery, R. B. (1938) *Pap. Phys. Oceanogr. Meteorol.* **6**(2).
4. Schroeder, E. H. (1965) *Deep-Sea Res.* **12**(3), 323–343.